

Towards a Robotic System for Minimally Invasive Breast Interventions

Vishnu Mallapragada and Nilanjan Sarkar
Vanderbilt University
USA

1. Introduction

Breast cancer is the most common cancer among American women and is the third leading cause of cancer death in women (American Cancer Society, 2009). The risk of breast carcinomas is approximately 1 in 8 women (Pass et al., 2008). As a result of nationwide implementation of screening for breast cancer, the proportion of small carcinomas found at the time of treatment has increased (Elmore et al., 2005). For small lesions, the standard of care is breast conserving therapy (BCT) with adjuvant radiation therapy (Arriagada et al., 2003). However, the cosmetic outcome of BCT is often disappointing with a satisfaction rate of 81% (Dian et al., 2007). Furthermore, BCT carries a relatively high morbidity rate due to bleeding (up to 11%) and infections (3.63%) (Bakker & Roumen, 2002; El Tamer et al., 2007). Breast asymmetry is also an issue with BCT where 35% of patients experience breast asymmetry after BCT (Dian et al., 2007).

The occurrence of benign epithelial lesions (e.g., fibroadenomas) is also common among women. Approximately 1 in 10 women experience a fibroadenoma in their lifetime (Rewcastle, 2005). As with BCT for carcinoma, surgical resection, the treatment of choice, provides definitive diagnosis, eliminates patient anxiety and reduces the need for follow-up monitoring, but it is expensive, can cause cosmetic or ductal damage and may be unnecessary because of the benign nature of the lesion (Greenberg et al., 1998). Additionally, it has been argued (Greenberg et al., 1998) that surgical resection of every fibroadenoma would place a huge burden on the health care system.

Because of bleeding, infection, cost and cosmetic considerations, several minimally invasive ablative therapies for breast carcinomas as well as benign fibroadenomas are being currently investigated that include cryoablation, radiofrequency ablation (RFA), laser-induced thermal therapy, microwave ablation and focused ultrasound (Van Esser et al., 2007). We present a brief background of cryoablation and RFA in order to motivate the need for development of a robotic breast intervention system.

Cryoablation is a very promising ablation technique to treat small breast tumors. It involves the introduction of a cryoprobe (about 2.4-3 mm in diameter) into the center of a tumor under ultrasound guidance in order to freeze the tissue to temperatures between -160°C and -190°C to kill the tumor cells (Sabel, 2008). Cryoablation is a simple and safe procedure with minimal discomfort or side effects for the patients (Whitworth & Rewcastle, 2005). After

percutaneous US (ultrasound) guided placement of the probe at the center of the tumor, the procedure involves monitoring the formation of an iceball and occasionally injecting saline between the iceball and the skin to prevent thermal damage. After (generally) two freeze-thaw cycles, the probe is removed and a bandage is placed over the incision. No local or regional anesthesia is needed past the probe placement, since freezing produces the same effect. Several small studies (Sabel et al., 2004; Pflaiderer et al., 2002; Staren et al., 1997; Morin et al., 2004) have demonstrated the safety, feasibility, efficacy and limitations of cryoablation for treating breast cancer. Data from these studies, most of which involve cryoablation followed by surgical resection, demonstrate that cryoablation was successful in destroying 100% of cancers less than 1 cm. For tumors between 1.0 and 1.5 cm, this success rate was achieved in patients with invasive ductal carcinoma without a significant ductal carcinoma-in-situ (DCIS) component. Cryoablation was not recommended for tumors greater than 1.5 cm. From these experimental results, it was concluded (Sabel, 2008) that cryoablation can safely and efficiently treat primary breast cancers. It can be performed in an office-based setting with only local anesthesia, and with minimal side effects or discomfort by a skilled practitioner.

Cryoablation has also been applied in treating benign breast tumors such as fibroadenomas (Kaufman et al., 2002; Kaufman et al., 2004). In recent years cryoablation has been an approved treatment by the US Food and Drug Administration for women with biopsy-proven fibroadenomas. There is another important application of cryoablation, which is cryoprobe-assisted lumpectomy (CAL). The gold standard for localization in mammographically-guided breast biopsy is needle wire localization (NWL). While NWL has high degree of diagnostic accuracy, it is less reliable in localizing malignant tumors prior to excision (Fornage & Edeiken, 2005). NWL is often ineffective at assuring a tumor-free margin in the specimen resulting in 20-79% re-excision rate (Rewcastle, 2005). In CAL, a cryoprobe is guided using US into the center of the tumor. The cryoprobe is engaged until an iceball is created that encloses not only the entire tumor but also a margin. The iceball enclosing the tumor is then surgically excised, which may prove to be a superior localization methodology than NWL (Tafra et al., 2003).

US-guided RFA, on the other hand, uses thermal energy to induce thermal tissue necrosis in the target region and is considered one of the most promising ablation techniques in the treatment of breast cancer (Noguchi, 2007). The diameter of RFA probes is similar to those of cryoablation except that the electrodes may have secondary prongs. The goal of RFA of primary breast cancer is to achieve a lethal thermal lesion that encompasses not only the tumor, but also a margin of surrounding normal tissue to destroy possible peripheral microscopic disease. There have been several pilot and feasibility US guided RFA studies conducted in USA, Japan, France and Italy (Jeffrey et al., 1999; Izzo et al., 2001; Elliot et al., 2002; Burak et al., 2003; Hayashi et al., 2003; Fornage et al., 2004; Noguchi et al., 2006; Marcy et al., 2006). It was found that a small T1 carcinoma less than 2 cm was ablated between 95-100%. The ablation rate for T1-T2 tumors less than 3.0 cm was 90%. It is concluded from the above studies that RFA can be effective for well-localized tumors measuring less than 2 cm. The use of real-time sonography has been less effective in RFA because the margins of the tumor may be obscured by a diffuse area of hyperechogenicity. Thus, the role of sonographic guidance in RFA is to ensure that the probe is placed right at the geometric center of the tumor.

Thus, in order to evaluate the clinical efficacy of these ablative procedures, they first need to be performed accurately. In addition, clinicians across the country should be able to perform them otherwise the benefits of these treatments will be limited to a few at specialized cancer centers. Naturally the question arises whether there is variability among the clinicians, which if it exists will adversely affect the use of such ablative procedures. Measuring, monitoring, and regulating the quality of breast surgery are controversial subjects (Schachter et al., 2006). Up to 90% of breast surgery in the US is provided by 25% of surgeons (Pass et al., 2008) and many surgeons perform surgery on fewer than 5 breast cancer patients annually (Neuner et al., 2004). For example, the numbers for lumpectomy per year are (Pass et al., 2008): 50% of surgeons do 2; 25% do 6; 10% do 11; and 1% do 34. Quality discrepancy has been noted in many studies and appears to be related to surgeon volume and/or specific breast surgery or surgical oncology training (Skinner et al., 2003). It is concluded by Pass et al. (2008) that breast-focused surgeons are more competent than the 50% of surgeons who do the occasional case. There is data to suggest that breast-focused surgeons have better outcome. For example, treatment by surgical oncologists resulted in 33% reduction in the risk of death at 5 years (Skinner et al., 2003). Possible reasons for such improved outcome include a volume effect, improved surgical techniques or appropriate use of multidisciplinary approach to cancer treatment (Skinner et al., 2003). However, it is likely that only approximately 10% of patients in the United States are treated by surgeons who perform at least 30 annual operations (Neuner et al., 2004). Variability also exists among radiologists (Woodward et al., 2007). For example, only 10% of all radiologists are breast imaging specialists but 61% of radiologists interpret mammograms, and only 30% of mammograms are interpreted by breast imaging specialists (Lewis et al., 2006). It was found that radiologists in academic medical centers, compared with other radiologists, had a higher sensitivity during interpretations. More training in mammography and more experience in performing breast biopsy were associated with a decreased threshold for recalling patients, resulting in statistically significant increases in sensitivity and false-positive rates (Miglioretti, 2007). The above discussion suggests that the variability among clinicians might adversely impact the clinical usefulness of cryoablation and RFA because of the requirement of the highest order of eye-hand coordination and may serve as a deterrent for their widespread use, notwithstanding the substantial benefits they can offer in terms of patient comfort, cosmetic results and cost.

Therefore, given the large variability that exists among breast clinicians (Pass et al., 2008; Schachter et al., 2006; Neuner et al., 2004; Skinner et al., 2003; Woodward et al., 2007; Lewis et al., 2006; Miglioretti et al., 2007), an automated system that can help the clinicians access small lesions in a precise manner for treatment without requiring the highest level of eye-hand coordination will likely be clinically useful, especially in community hospitals where a highly skilled radiologist-mammography specialist is less likely to be available. We therefore propose a new robotic technology for precise percutaneous probe placement to enhance the efficacy of minimally invasive ultrasound (US) guided ablative therapies such as cryoablation and radio frequency ablation (RFA) in the breast so that their scope and clinical usefulness can be effectively explored. In addition, this technology will offset clinician variability to a great extent and as a result, will help spread the use of ablative therapies in the breast to communities where such treatment might not otherwise be available.

Robotic technology has become sufficiently mature in recent years to be useful in many medical applications. There are numerous examples of these systems currently in use, such as the da Vinci Surgical System (Intuitive Surgical®). However, robotic aids are noticeably absent for breast surgery due to several unique technical challenges that are yet to be solved. In this work we will address two primary technical challenges to develop a novel robotic system for breast ablative procedures. These are: 1) how to ensure precise placement of a therapy delivery probe at the center of the tumor; and 2) how to minimize difficulty of ablative procedures. A robotic system that addresses these challenges will allow clinicians to precisely and easily access center of the breast lesion for therapeutic purposes.

In this chapter, the following terminology is used: target refers to a suspected lesion/tumor that is to be ablated; probe/needle (used interchangeably since the system development is independent of the specific instrument used to access the targets) refers to a treatment or therapy probe inserted into the target for ablation; US probe is the imaging probe used for acquiring US images.

2. Background and Literature Review

As mentioned before, there are two major problems to be addressed to improve the accuracy and reduce the difficulty of precise probe/needle placement at the center of the target.

Accurate needle placement: During needle insertion, the complex tissue of the breast induces the small target to deflect away from its original location. Figure 1 (DiMaio & Salcudean, 2003) shows a three dimensional (3D) finite element model of needle insertion in soft tissue. We can see from Figure 1 that as the needle is inserted, large tissue deformation causes the target to move away from the line of insertion of the needle. Other factors such as patient movement and breathing also cause inaccuracy in needle-target alignment. Note that accurate needle placement has to be achieved with a single insertion, since multiple insertions cause other risks such as excessive bleeding, tissue damage and significant patient discomfort.

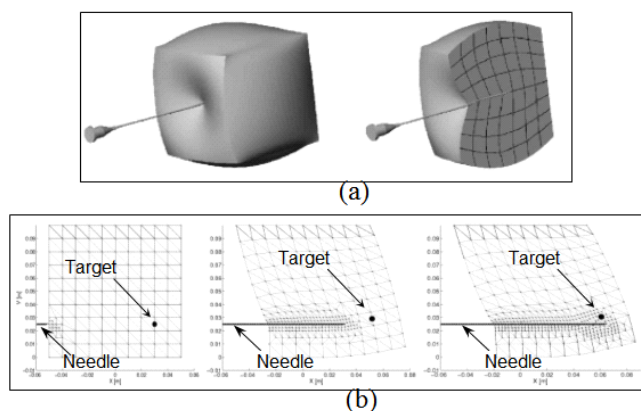


Fig. 1. Finite element model of needle insertion in soft tissue (DiMaio & Salcudean, 2003).

(a) Cross section of 3D model shows the finite element mesh.

(b) Target movement during needle insertion.

Difficulty of operation: Sonography is the widely used imaging technique because of its real-time capability and cost-effectiveness (Lieberman et al., 1998). The current state-of-the-art US guided technique is highly dependent on the skill of the clinician (Fornage, 1999). A clinician performs this procedure by holding the US probe with one hand and inserting the needle with the other hand. Since sonography only provides a 2D image, if the target moves out of plane of the transducer, the clinician has to continuously reorient the probe to keep the needle and the target in the imaging plane while inserting the needle. It is critical to orient the imaging plane parallel to the needle. This freehand procedure requires excellent hand-eye coordination. Since stabilization of the breast is problematic (Smith et al., 2001) and steering of the needle inside the breast is extremely difficult, many insertion attempts are required to successfully position the needle at the target. This procedure is very fatiguing for the clinician and uncomfortable for the patient.

To address such challenges, several groups have designed robotic systems to improve the accuracy of needle insertions (Cleary et al., 2006; Tsekos et al., 2001; Stoianovici et al., 1998; Cleary et al., 2001; Patriciu et al., 2001; Stoianovici et al., 2001). The reader is referred to the work of Cleary et al. (2006) for a detailed review of state-of-the-art in interventional robotic systems. Several systems, such as, a device for conditioning of the breast and positioning of the probe (Tsekos et al., 2001), robotic systems for needle insertion (Stoianovici et al., 1998), precise intratumoral placement of therapeutic agents (Cleary et al., 2001), spinal (Patriciu et al., 2001) and renal (Stoianovici et al., 2001) percutaneous procedures have been developed. "Although these innovations greatly improve accuracy by automating needle target alignment, they do not provide active trajectory correction in the likely event that trajectory errors arise" (Okazawa et al., 2005). Needle trajectory errors and target mobility result in multiple insertions at the same site for accurate needle placement.

As a result, significant research effort is being made to investigate techniques that can address the problem of target movement during needle insertion. Okazawa et al. (2005) and other researchers (Glozman et al., 2007; Webster III et al., 2006; Sears & Dupont, 2006) presented steerable devices that allow the clinician to steer the tip of the needle towards the target during insertion. With such a device the clinician would have to manoeuvre the needle using one hand with image data from a US monitor while at the same time correctly orienting the US probe and stabilizing the breast with the other hand. As mentioned earlier, such a freehand technique is extremely difficult (due to high level of hand eye coordination required) and fatiguing for the clinician and uncomfortable for the patient. A visually controlled needle-guiding system is developed by Loser & Navab (2000) for automatic or remote controlled percutaneous interventions. In the automated mode, needle insertion path is updated based on image feedback to the needle-guiding system. Azar et al. (2002) and Alterovitz et al. (2003) developed a finite element model of the breast to predict the movement of the target. The needle path is planned based on this prediction to accurately position the needle at the target. To get an accurate prediction of the movement of the target, finite element analysis requires the geometric model and mechanical properties of the breast. In addition, average time for computation is 29 minutes (Azar et al., 2002).

The goal of the current research is to address the problem of ensuring precise placement of the probe/needle at the target for minimally invasive breast procedures leading to the design and development of an innovative robotic breast intervention system to aid the clinician. This system will potentially allow the clinician to solely focus on the detection, decision making, and ablation of the target without being encumbered by the difficulty of

achieving good targeting accuracy. In addition, the system also facilitates breast stabilization, US image acquisition and processing. It is evident from the literature review that there does not currently exist such a system. The robotic system provides a mechanism to compensate for needle–target misalignment for providing access to mobile targets. A novel approach termed, “target manipulation”, (Mallapragada et al., 2008) is used to position the target inline with the needle thereby minimizing error in needle–target alignment. In this approach multiple robotic fingers manipulate the tissue externally to position a target inline with the needle during insertion.

In the following sections, basic theoretical framework of target manipulation is presented. Simulations and experimental results on phantoms are used to demonstrate the efficacy of this technique. Some aspects relating to the development of an autonomous US imaging system for minimizing difficulty of breast interventional procedures are also presented. The chapter ends with a discussion on the potential advantages and limitations of this system.

3. Control Framework

3.1. Noncollocated Controller for Target Manipulation

During image guided breast intervention a clinician inserts the needle through an incision in the skin. A schematic of needle insertion in a breast is shown in Figure 2.

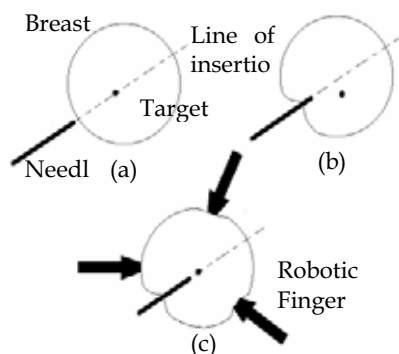


Fig. 2. Needle insertion schematic. (a) and (b) Target movement during needle insertion. (c) Minimizing needle – target misalignment using external robotic fingers.

The two dimensional plane of the figure represents a horizontal plane passing through the target. In the figure, a simplified anatomy for the breast is shown. In reality, breast tissue is inhomogeneous and its biomechanical properties are nonlinear. Hence, if the tip of the needle reaches the interface between two different types of tissue, its further insertion will push the tissue, instead of piercing it, causing unwanted deformations. These deformations move the target away from its original location, as shown in Figure 2b. In this section, we discuss controller design for the external robotic fingers positioned around the breast as illustrated in Figure 2c. These fingers apply forces on the surface of the breast based on the image of the target to guide the target towards the line of insertion of the needle.

During an interventional procedure, the needle is inserted into the breast at a shallow angle (away from the chest wall) to the horizontal plane containing the target. The needle incision

site and the orientation of the needle are chosen by the clinician considering factors such as location of target, location of critical anatomical structures and ease of access to target. The desired target position is the point where the line of insertion (of the needle) intersects the plane containing the target. While one can choose any plane that contains the target and has an intersection with the line of needle insertion, we choose this plane to be the horizontal plane for simplicity. The desired target position is determined by a planner based on the actual target location and needle direction. Note that we only need to control the target position in two dimensions (horizontal plane) to be able to successfully position the target along the line of insertion of the needle. Our goal is to design a controller that acts on the position error to guide the target towards the desired location. The controller is designed such that the effect of needle force (disturbance) on target position is minimized.

Before we discuss the design of the control system, we present a result by Wada et al. (2001) to determine the number of robotic fingers required to position the target at an arbitrary location in the horizontal plane. The following definitions are given according to the convention of Wada et al. (2001).

Manipulation points: Defined as the points that can be manipulated directly by robotic fingers. In our case, the manipulation points are the points where the external manipulators apply forces on the breast.

Positioned points: Defined as the points that should be positioned indirectly by controlling manipulation points appropriately. In our case, the target is the positioned point.

The control law to be designed is non-collocated since sensor feedback is from the positioned points and control force is applied at the manipulation points. The following result is useful in determining the number of fingers required to accurately position the target at the desired location.

Result (Wada et al., 2001): The number of manipulated points must be greater than or equal to that of the positioned points in order to realize any arbitrary displacement.

In our case, the number of positioned points is one, since we are trying to control the position of just the target. Hence, ideally the number of contact points would also be one. But practically there are two constraints: (1) We do not want to apply shear force on the breast to avoid damage to the skin. (2) We can only apply control forces directed into the breast. We cannot pull the skin on the breast since the robotic finger is not attached to the breast. Thus our problem becomes more restrictive since we need to control the position of the target by applying only unidirectional compressive force.

However, there exists a theorem on force direction closure in Mechanics that helps us determine the equivalent number of normal compressive forces that can replace one unconstrained force in a 2D (horizontal) plane.

Theorem (Nguyen, 1986): A set of wrenches W can generate force in any direction if and only if there exists a three-tuple of wrenches $\{W_1, W_2, W_3\}$ whose respective force directions f_1, f_2, f_3 satisfy:

(i) Two of the three directions f_1, f_2, f_3 are independent.

(ii) A strictly positive combination of the three directions is zero,

$$\alpha f_1 + \beta f_2 + \gamma f_3 = 0. \quad (1)$$

The ramification of this theorem for our problem is this: we need three control forces distributed around the breast (as shown in Figure 1c) such that the end points of their

direction vectors draws a non-zero triangle that includes their common origin point. With such an arrangement we can realize any arbitrary displacement of the target point.

To develop a control law for the robotic fingers, the breast is modeled as a discrete three dimensional network of mass-spring-dampers. Following the notation of McClamroch (1985), dynamics of the system can be written in the form

$$M\ddot{x} + F(x, \dot{x}) = Bf. \quad (2)$$

x , \dot{x} and \ddot{x} (variables in italics represent vectors) denote generalized displacement, velocity and acceleration vectors, respectively. Each of these vectors has size $2n \times 1$ where n is the number of nodes in the discretized model. M is a constant symmetric, positive definite mass matrix. F is a flexible nonlinear restoring force function. B is the influence matrix which links the location of the fingers to the geometry of the structure. f denotes a vector of the external force applied on the system. f is a combination of the control force f_c and the needle force f_n . The output displacement vector is defined as follows:

$$y = Cx. \quad (3)$$

Here, y is the position of the target and C is the output matrix. The output position data is obtained through image feedback. Let p_i ($i=1,2,3$) denote displacement of the manipulation point in contact with actuator i along the direction of actuation. We now define the displacement vector of the manipulation points as

$$p = [p_1 \ p_2 \ p_3]^T. \quad (4)$$

Note that the elements of p are also elements of x . We have performed extensive simulations to determine the nature of the control laws that would be appropriate for this control problem. In particular, we investigated three generic class of controllers: adaptive controller, force feedback controller and a proportional-integral (PI) position error-based controller.

Adaptive control:

$$\dot{f}_c = K_h (-\dot{p} + g^s y_d - g^d p - g^f f_c). \quad (5)$$

Here, f_c - force applied by the fingers, K_h - compliance matrix, \dot{p} - velocity vector of manipulation points, y_d - desired position of target, g^f , g^d - force and position feedback gain matrices, g^s - feedforward gain.

To drive the steady state error to zero, the feedforward gain g^s is selected based on the stiffness of the system (McClamroch, 1985). Since stiffness of the breast is unknown, feedforward gain is adaptively estimated using MIT rule. Adaptation law is given by

$$\dot{g}^s = -\nu (y_d - y) y_d', \quad (6)$$

where ν is the adaptation gain.

Force feedback control:

$$\dot{f}_c = K_h \{-\dot{p} + g^i \int (y_d - y) dt - g^d p - g^f f_c\}. \quad (7)$$

g^i is the integral gain. Instead of adaptively estimating the feedforward gain in (5), an integral term is added to eliminate steady state error.

PI control:

$$f_c = \{K_p(y_d - y) + K_i \int (y_d - y) d\tau\}. \quad (8)$$

K_p and K_i are proportional and integral gains. Note that in control laws (5), (7) and (8), geometric or mechanical properties of the breast are not required. Equations (2) and (3) are presented to develop a discretized model of the breast using a network of mass-spring-dampers. These equations (and consequently any model parameters) are not used in developing the control scheme. Equations (2) and (3) are used in simulation to construct a model of the breast for testing the feasibility of such a control methodology.

The implicit assumption in the control laws is that there exists kinematic coupling between the contact points and the target. This means that applying external control force (at the contact point) in a particular direction causes the target to move in a direction that has positive projection along the direction of force. Moreover, this assumes that the internal elastic force around the target can be controlled by applying external force on the surface. This assumption is valid since breast tissue is a continuous medium, however inhomogeneous. Inhomogeneity might cause the target to deflect away from the direction of force application, but continuity of the medium ensures kinematic coupling. Weak coupling (when the target is located away from the line of action of the fingers or due to inhomogeneity in the tissue) may necessitate large external forces to position the target but theoretically this does not undermine the control framework. Large external forces are undesirable so as to prevent patient injury and discomfort. This can be avoided in two ways: (1) appropriate positioning of the external fingers such that their line of action is close to the target; and (2) since breast tissue is not inhomogeneous in all directions, this problem can also be obviated by distributing the actuators around the breast. The theorem and result discussed above inherently address this problem and as an obvious consequence, the actuators are positioned 120° apart (in Figure 2c).

3.2. Simulation of Target Manipulation in Soft Tissue

Figure 3 shows a schematic of the control structure. Target position data (y) is obtained through image feedback. The desired target position (y_d) is determined by the planner based on the current target location and needle direction. The desired target position is always along the line of insertion of the needle. The controller acts on the position error and drives the robotic fingers to position the target at the desired location. The force exerted by the needle is the disturbance to the system.

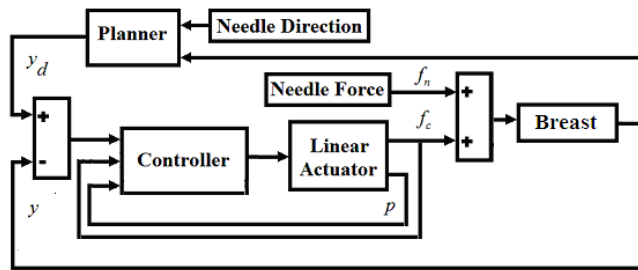


Fig. 3. Control structure.

To test the performance of the controllers, we simulated a needle insertion task using a 3D model of the breast. The target is located inside the breast and is initially at the origin of the coordinate system. A needle is inserted into the breast along the line specified by spherical coordinates: azimuth (θ) 45° , zenith (ϕ) 45° and passing through the origin. A plot of the needle insertion force is shown in Figure 4. The force profile is based on the elasto-plastic friction model (Yang et al., 2005). The insertion force gradually increases after contact with the breast surface (Point A to Point B). At Point B, the needle punctures the tissue characterized by a sudden drop in force (Point B to Point C). As the insertion continues, needle force steadily rises (Point C to Point D) mainly due to friction between needle and the tissue. Force remains constant once the insertion stops. In reality, there is a slight drop in force at Point D due to expansion of tissue. However, this drop in force is small and does not alter the results of this simulation significantly. In addition, force vibrations caused by the internal structure of the tissue have not been modeled since they do not significantly affect our results.

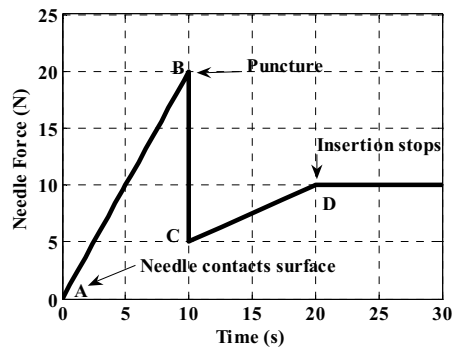


Fig. 4. Needle insertion force.

Figure 5 shows a plot of the trajectory of the target using the three different control laws. In Figure 5, Point A (origin) is the initial location of the target. The needle is inserted along the direction indicated by the broken arrow. As the needle is inserted, inhomogeneity in the tissue causes the target to move away from the needle path. As we can see from Figure 5, all three controllers successfully bring the target back to the needle path. The final target

location is at Point B which lies on the line of needle insertion. The simulation results suggest that adaptive controller and force feedback controller do not provide any significant advantage over the PI controller. Hence, a PI position error-based controller is chosen for this application since it is the cheapest and simplest controller with acceptable performance. Note that Figure 5 only shows the line of insertion of the needle and not the path of the needle. Temporal coordination of needle insertion and target manipulation has to be performed by the clinician through visual feedback from real time ultrasound imaging.

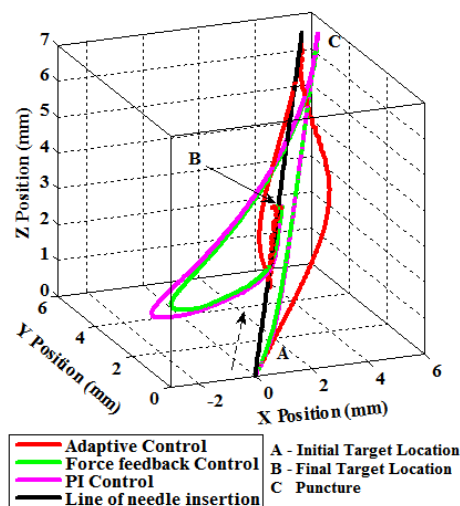


Fig. 5. Target trajectory.

4. Results

4.1. Phantoms

Deformable plastic phantoms with a stiff inclusion (a plastic insert placed in the phantom to mimic a tumor) are created to test the efficacy of the PI controller in positioning the inclusion at a desired location. We make the phantoms in such a manner that their material properties closely resemble breast tissue properties as published in the literature (Wellman, 1999). This step is necessary to ensure the success of the controller when it is applied to real breast tissue. The phantom is a cylindrical structure (radius 60mm, height 35mm) made of PVC (Poly Vinyl Chloride) plastic. The inclusion is a plastic sphere (radius 14 mm) that is much stiffer than the phantom. The inclusion is used as the target in the following experiments. Softening and hardening material is added to this plastic to alter its elastic property. Three phantoms (A, B, and C) are prepared with different mix ratios. Phantom A has plastic to hardener ratio of 4:1. Phantom B does not contain softener or hardener. Phantom C has plastic to softener ratio of 3:1. Procedure for preparing the phantoms is outlined by Mallapragada et al. (2007). The three phantoms are homogeneous.

Uniaxial compression tests are performed on each of the phantoms to determine their elastic properties. Nominal stress – strain values are computed from force – displacement data measured during the compression test. Elastic moduli of the phantoms are determined by

an exponential fit of the stress – strain curve (Wellman, 1999). Using the notation by Wellman (1999), stress – strain relationship is given by

$$\sigma_n^* = \frac{b^*}{m^*} (e^{m^* \varepsilon_n} - 1), \quad (9)$$

where σ_n^* is the nominal stress and ε_n is the nominal strain. b^* and m^* are the exponential fit parameters. The Young's modulus is given by

$$E = b^* e^{m^* \varepsilon_n}. \quad (10)$$

Figure 6 shows a plot of the Young's moduli of the phantoms. Fat tissue data shown in Figure 6 is presented by Wellman (1999). From the figure we can see that the phantoms have Young's moduli similar to that of fat tissue in the breast. Breast tissue properties vary greatly based on factors such as age, presence of tissue abnormality etc. In order to demonstrate feasibility of our technique under significant parameter variation, we prepared phantoms with varying elastic properties to demonstrate that the presented controller can work in realistic scenarios.

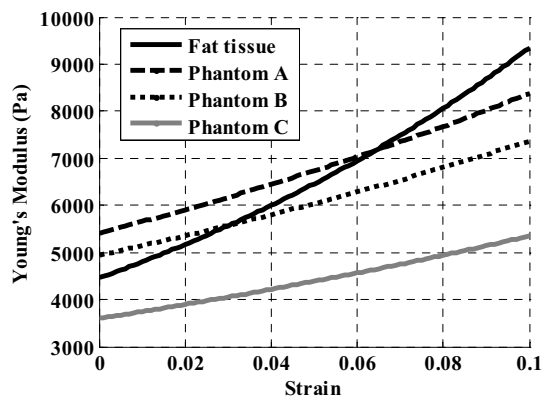


Fig. 6. Comparison of Young's modulus of fat tissue and phantoms.

4.2. Experimental Results

We demonstrate efficacy of this technique through planar manipulation experiments. In these experiments needle is inserted in the plane of target manipulation. Therefore, we only need two control forces (fingers) to position the target inline with the needle. When the needle is inclined to the plane of target manipulation, we will need three control forces (fingers) to position the target on the needle path. This is because when the needle is in the plane of target manipulation, the intersection between the axis of the needle and the plane is a line whereas when the needle is inclined to the plane, the intersection between the axis of the needle and the plane is a point. As discussed in Section 3.1, in either case planar manipulation is sufficient to position the target inline with the needle. Hence, results presented in this Chapter also demonstrate feasibility for out of plane needle insertion since in either case we are manipulating target position in the plane.

We have performed four different experiments to demonstrate different aspects of target manipulation. Needle used in the following experiments is a 10-gauge vacuum assisted device.

Experiment 1: In the first experiment, we demonstrate movement of the target during planar needle insertion. The phantoms used for this experiment are inhomogeneous (as is actual breast tissue) such that during needle insertion the target deflects away from the path of the needle. Figure 7 shows two images grabbed from the video signal during needle insertion. Figure 7a shows the initial target location prior to needle insertion. Figure 7b shows needle inserted along Y axis. As the needle is inserted, the target deflects away from the needle path.

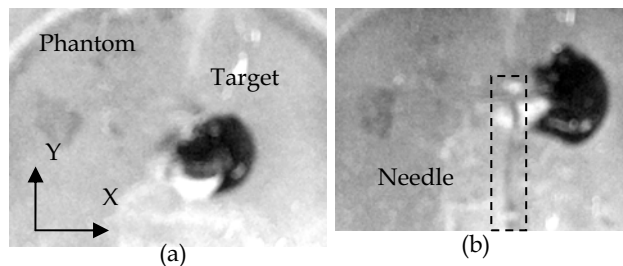


Fig. 7. Images grabbed from the video signal during needle insertion in inhomogeneous phantom. (a) Initial position of target in phantom is shown. (b) Displacement of target from needle path. Needle is identified in the figure with a dotted bounding box.

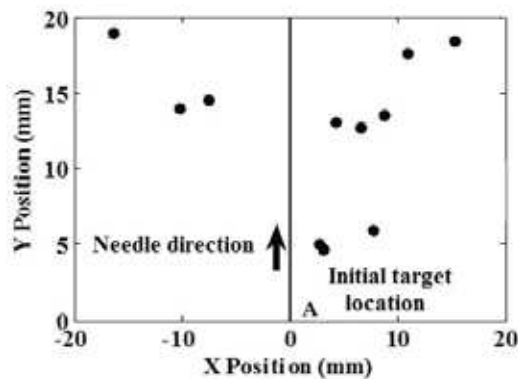


Fig. 8. Movement of target during needle insertion. Needle is inserted along Y axis. Dots indicate maximum displacement of target from the needle path.

Figure 8 shows a scatter plot of the maximum deflection of the target away from the needle path during multiple trials using different phantoms. Point A (origin) is the initial location of the target before the needle is inserted. The arrow indicates the direction of needle insertion. During 11 trials, the average maximum deflection of the target away from the needle path is 8.51 mm. The cone angle for target deflection ranges from 28.80 to 52.30.

These results are consistent with the observation of DiMaio & Salcudean (2003). Thus this experiment demonstrates that the phantoms that we have created behave similar to breast tissue.

Experiment 2: An experimental setup is constructed to test the efficacy of PI controlled robotic fingers in positioning the stiff target at a desired location by applying force on the surface of the phantom. A schematic of the experimental setup is shown in Figure 9.

The phantom is braced against a support on two sides and fingers apply force from the opposite sides. Position feedback is obtained using a Creative Labs video camera (30 Frames per second, 640 X 480 pixels). The target can be viewed using a video camera since the phantom is transparent. Image data from the video camera is converted from RGB to $YCbCr$ color space. The phantom is placed against a red background and the target is blue in color. Hence, chrominance (C_B) is used to track the target in real-time. Image processing algorithm consists of the following steps: 1) region segmentation to extract the region of interest, 2) color space conversion to convert from RGB to $YCbCr$, 3) thresholding to differentiate the target from the background, 4) median filtering to remove noise, and 5) blob analysis to extract target centroid coordinates.

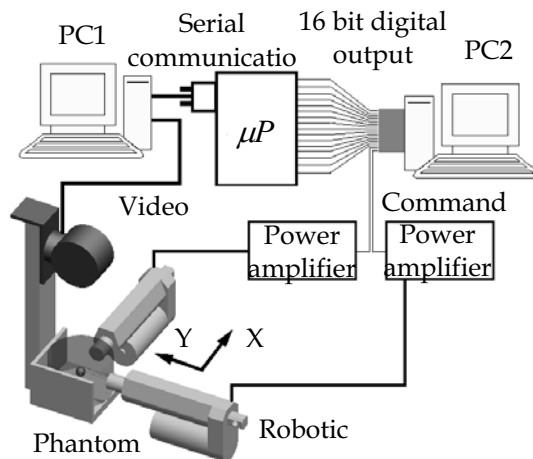


Fig. 9. Experimental setup shows system architecture and the location of actuators for target position control.

During an interventional procedure, image data would be obtained through ultrasound imaging. Image frames from the video camera are sent to a computer (1.6 GHz and 2 GB RAM, shown as PC 1 in Figure 9) running image processing algorithm in Matlab. Image frames are processed to extract position data of the target. Target position data is communicated serially to a microcontroller (Freescale 68HC912B32, 8 MHz clock frequency). The microcontroller outputs this data in a 16 bit parallel format. Each iteration of image processing and data communication requires 0.2 seconds. This is the time delay in the feedback loop of the controller. Medical US systems have frame rates of 5 frames per second

or higher. Hence the time delay in the feedback loop using US systems will be the same or less and the performance of the controller will not be affected. This data is read by another computer (1.6 GHz and 1GB RAM, shown as PC 2 in Figure 9) using a data acquisition card (Measurement computing PCIM DDA06/16). This computer runs the PI control algorithm and outputs control signals to power amplifiers for driving the robotic fingers. The fingers are lead screw driven linear actuators (FA-PO-20-12-2", Fircelli Automation) with inbuilt potentiometers. They have a no load speed of 50 mm/s and a load capacity of 88N at 25% duty cycle. The end-effector of the actuators has a circular surface area of 3.1 cm² (2 cm diameter). Contact between the end-effector of the finger and phantom is frictionless.

In this experiment, we have created a situation that is similar to the target deflection problem due to a needle insertion to demonstrate the feasibility of the concept. In a needle insertion situation, the task is to localize the target so that it remains inline with the needle. Any deviation of the target is seen as an error by the controller and a compensating force is generated to mitigate the error. We assume that the target is already deflected and the task of the controller is to move the target to a desired position by applying an external force. Thus this experiment is conducted to move the target to a desired location within the phantom using the fingers. Initial position of the target is set as the origin. Needle force acting as a disturbance on the system is not included for this experiment. This experiment is designed to move the target along two directions (X and Y axes as shown in Figure 9) using two fingers perpendicular to each other. The goal is to be able to position the target at any point in the horizontal plane (XY plane in Figure 9). Phantom is braced against a support opposite to the fingers.

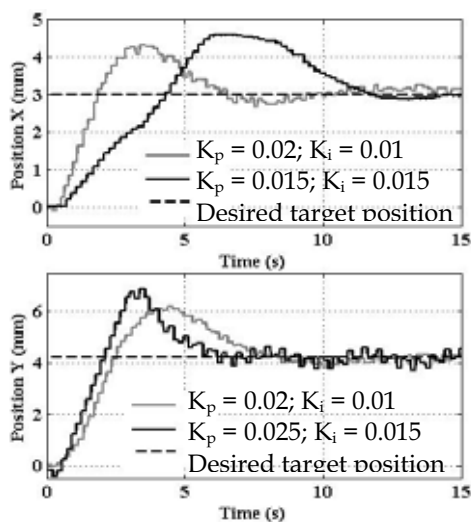


Fig. 10. Target positioning in horizontal plane. Position response of the target for two trials with different control gains. Target reaches the desired position in approximately 12 seconds with $K_p = 0.02$ and $K_i = 0.01$.

In PI control law (8), duty cycle of a PWM (Pulse Width Modulation) signal is used as actuator input instead of force. This is chosen to overcome friction based limit cycle behavior seen in DC (Direct Current) voltage controlled actuators. We use a PWM signal with frequency of 4 Hz and amplitude of 2 Volts for driving the fingers. The desired position of the target is 3 mm along X axis and 4.2 mm along Y axis. Two trials are performed with different sets of proportional and integral gains. For trial 1, proportional and integral gains are 0.02 and 0.01 respectively for both the actuators. For trial 2, proportional and integral gains are 0.015 and 0.015 (respectively) for the first finger (acting along X direction); proportional and integral gains are 0.025 and 0.015 (respectively) for the second finger (acting along Y direction). It can be observed from Figure 10 that the position response for trial 1 has less overshoot along both directions. For X direction, target reaches the desired position faster for trial 1. For Y direction, target response has less oscillation for trial 1. Therefore gains selected for trial 1 are better suited for target position control. It can also be observed from Figure 10 that the target reaches the desired position in approximately 12 seconds for trial 1. Note that any geometric or mechanical properties of the phantom are not used in the control scheme (8).

Experiment 3: For the third experiment, we use the robotic fingers to manipulate target position during a needle insertion task. The experimental setup for this task is shown in Figure 10.

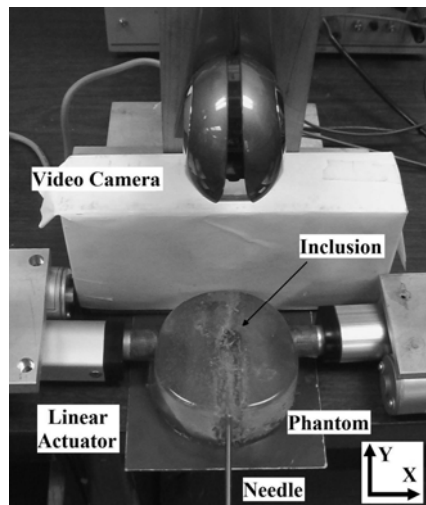


Fig. 11. Experimental setup for needle insertion task. Needle is inserted along Y axis. Robotic fingers control target position along X axis.

Target is initially located at the origin and the needle is inserted along the Y axis. Due to inhomogeneity in the phantom, target moves away from the needle path during insertion. We use fingers positioned along the X axis to steer the target towards the needle path (Y axis). During this experiment, force applied by the needle on the phantom is treated as a disturbance to the system. The task of the controller is to position the target on the Y axis

(needle path). Position of the target along Y axis is not controlled since the needle will intersect with the target no matter where it is located on the Y axis.

Figure 12 shows a plot of the position response of the target (along the X axis) during five trials (shown as Trials 1, 2, 3, 4 and 5) on three different inhomogeneous phantoms. The inhomogeneous phantoms are constructed by distributing the phantom material A, B and C (described in Section 4.1) in an asymmetrical arrangement during the molding process. These phantoms have two kinds of material with elastic moduli similar to fat and glandular tissue.

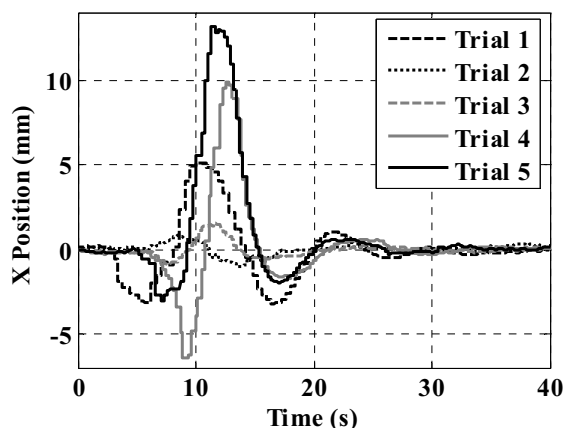


Fig. 12. Target position response during needle insertion. Plot shows that the target reaches the needle path in approximately 28 seconds.

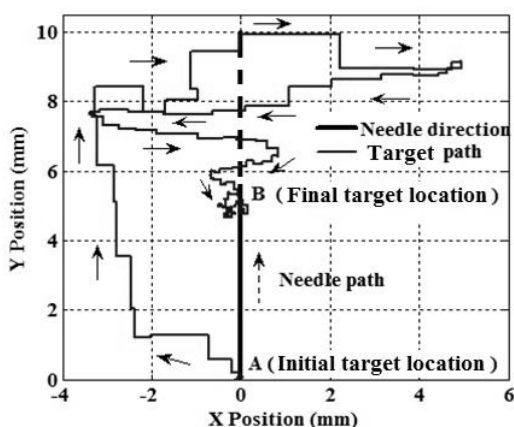


Fig. 13. Locus of target position for Trial 1. Needle is inserted along the Y axis. Point A is the initial target location and point B is the final target location.

From Figure 12, it can be observed that the target is initially located on the Y axis (displacement along X axis is zero). As the needle is inserted, target moves away from the Y axis (non zero displacement along X axis). This initiates a control action by the fingers, which steer and position the target on the Y axis (displacement along X axis is zero) at steady state. As we can see from Figure 12, target is steered back to the needle path in about 30 seconds. In all five trials, we were successful in positioning the target along the needle path. We could steer the target back to the needle path even when the deviation of the target is large (~10 mm).

Figure 13 shows locus of the target position for Trial 1. We can see from Figure 13 that the target is initially located in the path of the needle (Point A), but as the needle is inserted it deviates away from the path and the fingers (under PI control action) steer it back towards the line of insertion. The final location of the target is at Point B on the needle path.

Root mean square error (RMSE) is used to quantify the targeting accuracy of this technique. RMSE is defined as

$$RMSE = \sqrt{\frac{\sum_{t=t_i}^{t_f} (x_d - x)^2}{n}} \tag{11}$$

where t_i and t_f represent the limits of the time interval over which RMSE is computed.

x_d is the desired target position and x is the actual target position at time t . n is the number of data points in the chosen time interval. Table I shows the RMSE values for the five trials in Figure 12. In these trials the desired target position is along the Y axis, hence $x_d = 0$. Targeting accuracy needs to be evaluated when the target is positioned on the needle path, therefore steady state position data ($t_i = 30$ s; $t_f = 40$ s) is used to compute RMSE. The sampling time for the controller is 0.001 s, hence $n = 10001$. As we can see from Table 1, the targeting error in all cases is one order of magnitude less than the diameter of the needle (10-gauge, 3.4 mm). Therefore this technique can be used to successfully position the target on the needle path.

Trial #	1	2	3	4	5
RMSE (mm)	0.32	0.18	0.10	0.13	0.12

Table 1. Targeting accuracy with external manipulation

Experiment 4: We present results with a 2D US system to demonstrate applicability of this technique using US image feedback. The experimental setup is shown in Figure 14. Image feedback is obtained using a Toshiba ECCO-CEE (model SSA-340A) US system. US images are acquired using a frame grabber card (Data Translation, DT3120). Figure 15 shows an image grabbed from the video signal of the US system. Dark blob in the image is the target. Region segmentation, thresholding, median filtering and blob analysis are used to extract target position coordinates.

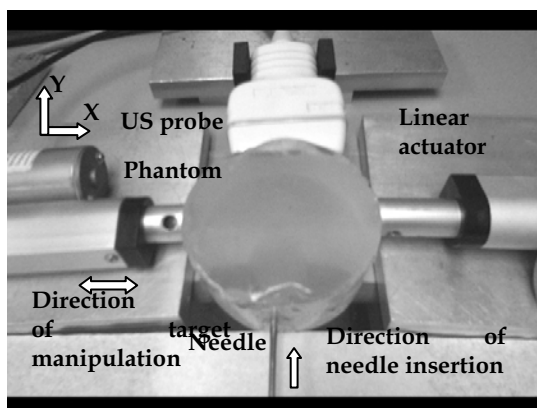


Fig. 14. US experimental setup. Needle is inserted along Y axis and fingers control target position along X axis.

The task description for this experiment is similar to Experiment 3. The target is initially located at the origin and the needle is inserted along the Y axis (Figure 14). We use robotic fingers positioned along the X axis to steer the target towards the needle path (Y axis). The task of the controller is to position the target on the Y axis. XY plane is the imaging plane of the US probe. In this setup, position of the actuators and needle (with respect to the US image space) are hard coded into controller.

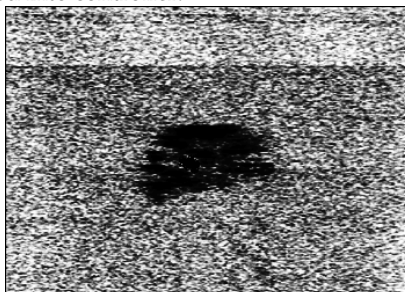


Fig. 15. US image of target in phantom. Dark blob in the image is the target.

Figure 16 shows the locus of target position. We can see from Figure 16 that the target is initially located in the path of the needle (Point A), but as the needle is inserted it deviates away from the path and the actuators steer it back towards the line of insertion. The final location of the target is at Point B on the needle path where it meets the needle. RMSE in this experiment is 0.06 mm.

During needle insertion, real-time video (rendered on US or computer monitor display) provides visual information of the position of the needle and target. In these experiments, operator controls needle insertion depth based on visual feedback so that the needle does not overshoot/cross the target location. If needle insertion is automated, target manipulation has to be coordinated with needle insertion so as to ensure alignment of the target with needle tip.

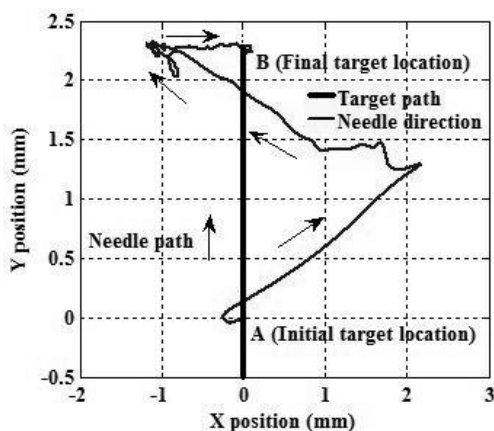


Fig. 16. Locus of target position for Experiment 4. Needle is inserted along the Y axis. Point A is the initial target location and point B is the final target location.

5. Autonomous US Imaging

Researchers have developed robotic systems to alleviate the difficulty associated with acquiring US images during medical procedures (Abolmaesumi et al., 2002; Masuda et al., 2001). Robotic systems with autonomous US imaging minimize the difficulty of breast interventions (Section 2) and also reduce the incidence of musculoskeletal disorders in sonographers. However, despite the potential advantages offered by robotic US imaging systems, there are some technical challenges that need to be overcome in order to realize autonomous US image acquisition.

2D US is the most widely used and cost effective clinical imaging technique. There are two major limitations of 2D US imaging. First, Tracking the location of a target (3D coordinates) using a 2D US probe requires knowledge of the position of the probe and coordinates of the target in the image plane of the probe. Sensors are used to measure the position of the probe. Coordinates of the target are extracted using an image processing algorithm, if the target is in the imaging plane. If the target is out of the imaging plane, there is uncertainty in determining the location of the target with respect to the imaging plane i.e., there is no information regarding the location of the target in a direction perpendicular to the imaging plane. Second, the US probe has to be continuously in contact with the surface of the breast to ensure acoustic coupling. Surface deformation due to target manipulation and needle insertion may result in the US probe losing contact with the breast. Loss of contact has to be detected (robotic systems use force sensors for detecting contact state of the US probe) and the US probe has to be moved to reestablish contact with the surface.

Even though the systems described in literature greatly reduce the difficulty of acquiring US images, the target cannot be tracked in real-time if it moves out of the imaging plane of the probe. Therefore, there is a need for a robust image acquisition system that is capable of automatic search and recovery of the target. Currently, none of the existing systems have this ability.

Real time automated target tracking using 2D US is a challenging task especially since US gives image of a two dimensional cross-section. We are investigating a system for

positioning the US probe guided by an image acquisition algorithm for automatic retrieval of the image of the target. This system continuously orients the transducer such that the 3D coordinates of the target are tracked in real-time. A novel sensorless technique for detecting contact state of US probe is also being investigated. The region in the image close to the edge (where the US probe makes contact with the surface) is used to detect the contact state of the US probe. This region is extracted from the US image and Otsu's method is used to estimate the greyscale threshold for the region. The threshold differential between contact and non contact states is used to infer the contact state of the US probe.

The target manipulation technique presented in this paper will be integrated with the autonomous US imaging system to provide comprehensive robotic assistance during US guided breast interventional procedures.

6. Discussion

PI control architecture has been presented in the paper for guiding a target towards the needle path. The performance of the controller is tested on phantoms with elastic property similar to that of breast tissue. We have demonstrated planar needle insertion as a proof-of-concept of a new control approach to target manipulation. As discussed in Section 4.2, it does not limit the scope of our results. Results show that PI controlled robotic fingers can be used to efficiently position a target inline with needle during insertion. The proposed technique of guiding breast interventions can increase the success rate of the procedure. The entire procedure is predicted to be fast, making it clinically viable. Since the needle is not steered inside the breast, tissue damage is also minimized. Additionally, since multiple insertions are not required, the proposed technique will likely reduce clinician fatigue and patient discomfort and improve the structural integrity of the tissue specimen. Geometric and mechanical properties of the breast are not required for precise positioning of the target. Target identification in ultrasound is a significant challenge and as such our work does not address this issue. The targets in our experiments are easily identifiable in the video frame. The focus of this paper is on developing a new targeting approach for breast interventional procedures which can be integrated with any real time imaging modality.

The proposed technique is not without limitations. In the experimental setup, position of the needle (with respect to the image space) is hard coded into the controller. However, this would be infeasible in a clinical setting. Therefore, needle position/orientation has to be measured using a 6 degree-of-freedom electromagnetic sensor, or estimated using needle segmentation techniques in US image.

The end-effector of the actuator has a circular cross section with 20 mm diameter. During experimental tests, we observed that maximum target movement in any direction is typically in the range of 5 - 10 mm. Since the end-effector has surface contact (contact area is 3.14 cm²), even if the target moves out-of-plane, the actuators can still control the target motion without causing instability. It is highly unlikely that target movement will be greater than 20 mm. If such an extreme case is observed, the robotic system requires another degree-of-freedom so that the actuators can move in a direction perpendicular to the plane of manipulation. However, issues relating to stability for out-of-plane target movements have not been investigated in this work.

7. Conclusion

We have presented a new paradigm for breast interventions that will allow the clinician to place the treatment probe at the center of a breast tumor for ablative procedures under real-time US image feedback and computer control. However, the clinician will have full control of the treatment probe. The robotic system will control the position of the tumor by careful manipulation of the breast such that the tumor centroid always remains along the line of insertion of the probe. Thus, this unique system will ensure that the probe placement is precise, and as a result, the effect of ablation is optimum.

There are several important benefits that can be derived from this technological innovation. **First**, it will enhance the clinical efficacy of cryoablation and RFA by allowing the clinician to place the probe precisely at the center of the tumor. It will help create an ablative zone that is expected to encompass the whole tumor with a given margin. As a result, one can analyze the clinical outcome of such procedures without the contribution of positioning error. **Second**, given the variability that exists among clinicians treating breast cancers and since ablation procedures require the highest level of eye-hand coordination skills, it is realistic to assume that most patients will not be benefited by this treatment option in its current form. The proposed robotic system will significantly reduce the eye-hand skill requirement on the part of the clinician and thereby will allow a majority of physicians to perform these ablative procedures all over the country. The proposed system will thus help decentralize breast cancer treatment to a certain extent and potentially reduce the load on breast cancer centers. Clinicians in community hospitals and private practice, who may not experience high volume or may not have specialized training, will feel comfortable in administering ablative procedures because the mechanical accuracy will be guaranteed by the robotic system. **Third**, by helping to perform these ablative procedures accurately (in terms of positioning of the probe) and thus allowing many more clinicians to perform these procedures, this robotic system is expected to contribute towards cost savings in healthcare, and improving cosmesis of patients. It has been predicted that by 2010, 50% of newly diagnosed breast cancers may be less than 1 cm (Cady, 2000). That would represent 90,000 patients for whom a lumpectomy will be necessary, with the associated operating room time, anesthesia, cost, and cosmetic and psychological impact (Sabel et al., 2004). If even a fraction of these patients could be helped by this system, the benefits will be substantial and would be a significant improvement to treatment of breast cancer.

8. Acknowledgment

The authors gratefully acknowledge the guidance of Dr. Tarun Podder (Jefferson University Hospital, Philadelphia) during the course of this work. The authors would also like to thank Dr. David Pickens (Radiology Imaging Research Laboratory, Vanderbilt University) for his support.

9. References

- Abolmaesumi, P., Salcudean, S.E., Zhu, W., Sirouspour, M.R., DiMaio, S.P. (2002). Image-guided control of a robot for medical ultrasound. *IEEE Transactions on Robotics and Automation*, Vol. 18, No. 1, pp. 11-23

- Alterovitz, R., Goldberg, K., Pouliot, J., Taschereau, R. & Hsu, I-C. (2003). Sensorless planning for medical needle insertion procedures. *Proc. of IEEE International Conference on Intelligent Robots and Systems*, pp. 3337 – 3343
- American Cancer Society (ACS): Cancer Facts & Figures, <http://www.cancer.org/downloads/STT/2008CAFFfinalsecured.pdf>, webpage accessed on February 2009
- Arriagada, R., Le, M.G., Guinebretiere, J.M., et al. (2003). Late local recurrences in a randomized trial comparing conservative treatment with local mastectomy in early breast cancer patients. *Annals of Oncology*, 14(11):1617-1622
- Azar, F.S., Metaxas, D.N. & Schnall, M.D. (2002). Methods for modeling and predicting mechanical deformations of the breast under external perturbations. *Medical Image Analysis*, Vol. 6, pp 1-27
- Bakker, X.R. & Roumen, R.M. (2002). Bleeding after excision of breast lumps. *Eur J Surg*, 168(7):401-403
- Burak, W.E. Jr., Agnese, D.M., Povoski, S.P. et al. (2003). Radiofrequency ablation of invasive breast carcinoma followed by delayed surgical excision. *Cancer*, 98:1369-1376
- Cady, B. (2000). Breast cancer in third millennium. *Breast J*, 6:280-287
- Cleary, K., Freedman, M., Clifford, M., Lindisch, D., Onda, S. & Jiang, L. (2001). Image-guided robotic delivery system for precise placement of therapeutic agents. *J. Controlled Release*, Vol. 74, No. 1, pp. 363–368
- Cleary, K., Melzer, A., Watson, V., Kronreif, G. & Stoianovici, D. (2006). Interventional robotic systems: Applications and technology state-of-the-art. *Minimally Invasive Therapy and Allied Technologies*, Vol. 15, No. 2, 101-113
- Dian, D., Schwenn, K., Mylonas, I., et al. (2007). Aesthetic result among breast cancer patients undergoing autologous breast reconstruction versus breast conserving therapy. *Arch. Gynecol. Obstet.*, 275(6):445-450
- DiMaio, S.P. & Salcudean, S.E. (2003). Needle insertion modeling and simulation. *IEEE Transactions on Robotics and Automation*, Vol. 19, No. 4
- Elliot, R.L., Rice, P.B., Suits, J.A. et al. (2002). Radiofrequency ablation of a stereotactically localized nonpalpable breast carcinoma. *Am Surg*, 68:1-5
- Elmore, J.G., Armstrong K., Lehman C.D., et al. (2005). Screening for breast cancer. *JAMA* 293(10):1245-1256
- El Tamer, M.B., Ward, B.M., Scifftner, T., et al. (2007). Morbidity and mortality following breast cancer surgery in women: national benchmarks for standard of care. *Ann Surg*, 245(5):665-671
- Fornage, B.D. (1999). Sonographically guided needle biopsy of nonpalpable breast lesions. *Journal of Clinical Ultrasound*, Vol. 27, No. 7
- Fornage, B.D., Sneige, N., Ross, M.I. et al. (2004). Small (less than equal to 2 cm) breast cancer treated with US-guided radiofrequency ablation: feasibility study. *Radiology*, 231:215-224
- Fornage, B.D. & Edeiken, B.S. (2005). Percutaneous ablation of breast tumors. In: *Tumor Ablation: Principles and Practice*, Vansonnenberg, E., Solbiati, L. & McMullen, W, 428-439, Springer-Verlag, ISBN 13:978-0387-95539-1, New York
- Glozman, D. & Shoham, M. (2007). Image-guided robotic flexible needle steering. *IEEE Transactions on Robotics*, Vol. 23, No. 3, pp 459 – 467
- Greenberg, R., Skornick, Y. & Kaplan, O. (1998). Management of breast fibroadenoma. *J Gen Intern Med*, 13:640-645

- Hayashi, A.H., Silver, S.F., Van Der Westhuizen, N.G. et al. (2003). Treatment of invasive breast carcinoma with ultrasound-guided radiofrequency ablation. *Am J Surg*, 185:429-435
- Izzo, F., Thomas, R., Delrio, P. et al. (2001). Radiofrequency ablation in patients with primary breast carcinoma. A pilot study in 26 patients. *Cancer*, 92:2036-2044
- Jeffrey, S.S., Birdwell, R.L., Ikeda, D.M. et al. (1999). Radiofrequency ablation treatment for breast cancer: first report of an emerging technology. *Arch Surg*, 134:1064-1068
- Kaufman, C.S., Bachman, B., Littrup, P.J. et al. (2002). Office-based ultrasound-guided cryoablation of breast fibroadenomas. *Am J Surg*, 184:394-400
- Kaufman, C.J., Littrup, P.J., Freman-Gibb, L.A. et al. (2004). Office-based cryoablation of breast fibroadenomas: 12-month followup. *J Am Coll Surg*, 198(6):914-923
- Lewis, R.S., Sunshine, J.H. & Bhargavan, M. (2006). A portrait of breast imaging specialists and the interpretation of mammography in the U.S. *Am J Roentgenol*, 187:W456-W468
- Liberman, L., Feng, T. L., Dershaw, D. D., Morris, E. A. & Abramson, A. F. (1998). US-guided core breast biopsy: use and cost-effectiveness. *Radiology*, Vol. 208, 717-723
- Loser, M.H. & Navab, N. (2000). A new robotic system for visually controlled percutaneous interventions under CT fluoroscopy. *Proc. of MICCAI*, Vol. 1935, LNCS, pp.887-896
- Mallapragada, V., Sarkar, N., Podder, T. (2007). A Robotic system for real-time tumor manipulation during image guided breast biopsy. *Proc. of IEEE International Conference on Bioinformatics and Bioengineering*, pp. 204-210
- Mallapragada, V., Sarkar, N., Podder, T. (2009). Robot assisted real-time tumor manipulation for breast biopsy. *IEEE Transactions on Robotics* (to be published)
- Marcy, P.Y., Magne, N., Castadot, P. et al. (2006). Ultrasound-guided percutaneous radiofrequency ablation in elderly breast cancer patients: preliminary institutional experience. *Br J Radiol*, 80(952):267-273
- Masuda, K., Kimura, E., Tateishi, N., Ishihara, K. (2001). Three-dimensional motion mechanism of ultrasound probe and its application for tele-echography system. *Proc. of IEEE/RSJ International Conference on Intelligent Robots and Systems*, pp. 1112-1116
- McClamroch, N.H. (1985). Displacement control of flexible structures using electrohydraulic servo-actuators. *Journal of Dynamic Systems, Measurement and Control*, Vol 107, pp 34-39
- Miglioretti, D.L., Smith-Bindman, R., Abraham, L. et al. (2007). Radiologist characteristics associated with interpretive performance of diagnostic mammography. *JNCI* 99(24):1854-1863
- Morin, J., Traore', A., Dionne, G., et al. (2004). Magnetic-resonance-guided percutaneous cryosurgery of breast carcinoma: technique and early clinical results. *Can J Surg*, 47:347-351
- Neuner, J.M., Gilligan, M.A., Sparapani, R., et al. (2004). Decentralization of breast cancer surgery in the United States. *Cancer*, 101:1323-1329
- Nguyen, V.D. (1986). Constructing force-closure grasps. *Proc. of International Conference on Robotics and Automation*, Vol. 3, pp. 1368 - 1373
- Noguchi, M., Earashi, M., Fujii, H. et al. (2006). Radiofrequency ablation of small breast cancer followed by surgical resection. *J Sur Oncol*, 93:120-128

- Noguchi, M. (2007). Is radiofrequency ablation treatment ready for “prime time”? *Breast Cancer Treat*, 106:307-314
- Okazawa, S., Ebrahimi, Chuang, J., Salcudean, S.E. & Rohling, R. (2005). Hand-held steerable needle device. *IEEE/ASME Transactions on Mechatronics*, Vol. 10, pp 285-296
- Pass, H.A., Klimberg, S.V. & Copeland, E.M. (2008). Are “Breast-Focused” surgeons more competent? *Annals of Surgical Oncology*, 15(4):953-955
- Patriciu, A., Solomon, S., Kavoussi, L. & Stoianovici, D. Robotic kidney and spine percutaneous procedures using a new laser-based CT registration method. *Proc. Of MICCAI*, Vol. 2208, pp.249-257
- Pfleiderer, S.O., Freesmeyer, M.G., Marx, C. et al. (2002). Cryotherapy of breast cancer under ultrasound guidance: initial results and limitations. *Eur Radiol*, 12:3009-3014
- Rewcastle, J.C. (2005). Application of cryoablation in breast, In: *Tumor Ablation: Principles and Practice*, Vansonnenberg, E., Solbiati, L. & McMullen, W, 423-427, Springer-Verlag, New York
- Sabel, M.S., Kaufman, C.S., Whitworth, P. et al. (2004). Cryoablation of early-stage breast cancer: work-in-progress report of a multi-institutional trial. *Annals of Surgical Oncology*, 11(5):542-549
- Sabel, M.S. (2008). Cryoablation for breast cancer: no need to turn a cold shoulder. *J Surg Onco*, 97:485-486
- Schachter, H.M., Mamaladze, V., Lewin, G., et al. (2006). Many quality measurements, but few quality measures assessing the quality of breast cancer care in women: a systematic review. *BMC Cancer*, 6:291
- Sears, P. & Dupont, P. (2006). A Steerable Needle Technology Using Curved Concentric Tubes. *Proc. of IEEE/RSJ International Conference on Intelligent Robots and Systems*, pp. 2850 - 2856
- Skinner, K.A., Helsper, J.T., Deapen, D., et al. (2003). Breast cancer: do specialists make a difference? *Ann Surg Oncol*, 10:606-615
- Smith, W.L., Surry, K.J.M., Mills, G.R., Downy, D.B. & Fenster, A. (2001). Three-dimensional ultrasound-guided core needle breast biopsy. *Ultrasound Med Biol*, Vol. 27, No. 8, pp. 1025-1034
- Staren, E.D., Sabel, M.S., Gianakakis, L.M. et al. (1997). Cryosurgery of breast cancer. *Arch Surg*, 132:28-33 discussion 34
- Stoianovici, D., Whitcomb, L., Anderson, J., Taylor, R. & Kavoussi, L. (1998). A modular surgical robotic system for image guided percutaneous procedures. *Proc. Of MICCAI*, Vol. 1496, LNCS, pp. 404-410
- Stoianovici, D., Cadeddu, J.A., Demaree, R.D. et al. (2001). A novel mechanical transmission applied to percutaneous renal access. *Proc. of ASME Dynamic Systems Control Division, DSC*, Vol. 61, pp. 401-406
- Tafra, L., Smith, S.J., Woodward, J.E. et al. (2003). Pilot trial of cryoprobe assisted breast-conserving surgery for small ultrasound visible cancers. *Ann Surg Oncol*, 10(9):1018-1024
- Tsekos, N.V., Shudy, J., Yacoub, E., Tsekos, P.V. & Koutlas, I.G. (2001). Development of a robotic device for MRI-guided interventions in the breast. *Proc. of Bioinformatics and Bioengineering Conference*, 201-208

- Van Esser, S., Maurice, A.A., Van Der Bosch, J., et al. (2007). Minimally invasive ablative therapies for invasive breast carcinomas: an overview of current literature. *World J Surg*, 31:2284-2292
- Wada, T., Hirai, S., Kawamura, S. & Kamiji, N. (2001). Robust manipulation of deformable objects by a simple PID feedback. *Proc. of International Conference on Robotics and Automation*, pp. 85-90
- Webster III, R.J., Kim, J.S., Cowan, N.J., Chirikjian, G. & Okamura, A.M. (2006). Nonholonomic modeling of needle steering. *International Journal of Robotics Research*, 25(5/6), pp. 509-526
- Wellman, P. (1999). *Tactile imaging*. PhD dissertation, Division of Engineering and Applied Sciences, Harvard University, Cambridge, Massachusetts
- Whitworth, P.W. & Rewcastle, J.C. (2005). Cryoablation and cryolocalization in the management of breast disease. *J Surg Oncol*, 90:1-9
- Woodward, D.B., Gelfand, A.E., Barlow, W.E., et al. (2007). Performance assessment for radiologists interpreting screening mammography. *Statist. Med.*, 26:1532-1551
- Yang, H., Liu, P.X., Zhang, J. (2005). Modelling of needle insertion forces for surgical simulation. *Proc. of International Conference on Mechatronics and Automation*, pp 592-595



Recent Advances in Biomedical Engineering

Edited by Ganesh R Naik

ISBN 978-953-307-004-9

Hard cover, 660 pages

Publisher InTech

Published online 01, October, 2009

Published in print edition October, 2009

The field of biomedical engineering has expanded markedly in the past ten years. This growth is supported by advances in biological science, which have created new opportunities for development of tools for diagnosis and therapy for human disease. The discipline focuses both on development of new biomaterials, analytical methodologies and on the application of concepts drawn from engineering, computing, mathematics, chemical and physical sciences to advance biomedical knowledge while improving the effectiveness and delivery of clinical medicine. Biomedical engineering now encompasses a range of fields of specialization including bioinstrumentation, bioimaging, biomechanics, biomaterials, and biomolecular engineering. Biomedical engineering covers recent advances in the growing field of biomedical technology, instrumentation, and administration. Contributions focus on theoretical and practical problems associated with the development of medical technology; the introduction of new engineering methods into public health; hospitals and patient care; the improvement of diagnosis and therapy; and biomedical information storage and retrieval. The book is directed at engineering students in their final year of undergraduate studies or in their graduate studies. Most undergraduate students majoring in biomedical engineering are faced with a decision, early in their program of study, regarding the field in which they would like to specialize. Each chosen specialty has a specific set of course requirements and is supplemented by wise selection of elective and supporting coursework. Also, many young students of biomedical engineering use independent research projects as a source of inspiration and preparation but have difficulty identifying research areas that are right for them. Therefore, a second goal of this book is to link knowledge of basic science and engineering to fields of specialization and current research. The editor would like to thank the authors, who have committed so much effort to the publication of this work.

How to reference

In order to correctly reference this scholarly work, feel free to copy and paste the following:

Vishnu Mallapragada and Nilanjan Sarkar (2009). Towards a Robotic System for Minimally Invasive Breast Interventions, *Recent Advances in Biomedical Engineering*, Ganesh R Naik (Ed.), ISBN: 978-953-307-004-9, InTech, Available from: <http://www.intechopen.com/books/recent-advances-in-biomedical-engineering/towards-a-robotic-system-for-minimally-invasive-breast-interventions>

INTECH
open science | open minds

InTech Europe

University Campus STeP Ri
Slavka Krautzeka 83/A

InTech China

Unit 405, Office Block, Hotel Equatorial Shanghai
No.65, Yan An Road (West), Shanghai, 200040, China

51000 Rijeka, Croatia
Phone: +385 (51) 770 447
Fax: +385 (51) 686 166
www.intechopen.com

中国上海市延安西路65号上海国际贵都大饭店办公楼405单元
Phone: +86-21-62489820
Fax: +86-21-62489821

© 2009 The Author(s). Licensee IntechOpen. This chapter is distributed under the terms of the [Creative Commons Attribution-NonCommercial-ShareAlike-3.0 License](#), which permits use, distribution and reproduction for non-commercial purposes, provided the original is properly cited and derivative works building on this content are distributed under the same license.